Novel Redox Chemistry of [3Fe−4S] Clusters: Electrochemical Characterization of the All-Fe(II) Form of the [3Fe−4S] Cluster Generated Reversibly in Various Proteins and Its Spectroscopic Investigation in *Sulfolobus acidocaldarius* Ferredoxin

Jillian L. C. Duff,[†] Jacques L. J. Breton,[‡] Julea N. Butt,[†] Fraser A. Armstrong,*[,†] and Andrew J. Thomson*[,‡]

Contribution from the Inorganic Chemistry Laboratory, South Parks Road, Oxford OX1 3QR, England, and School of Chemical Sciences, University of East Anglia, Norwich NR4 7TJ, England

Received May 3, 1996[⊗]

Abstract: The novel "hyper-reduced" form of protein-bound [3Fe−4S] clusters, which is *two electron equivalents* below the normal reduced form $[3Fe-4S]^0$ and thus formally composed entirely of Fe(II) subsites, has been characterized by electrochemistry and by EPR, MCD, and UV/visible spectroscopy. The two-electron reduction of $[3Fe-4S]^0$ has been studied for a range of proteins, in particular the 7Fe ferredoxins from *Sulfolobus acidocaldarius*, *Desulfovibrio africanus*, and *Azotobacter vinelandii*. In each case, the reaction is chemically reversible, the product is surprisingly inert, and the pH-dependent reduction potential is in the region of −700 mV vs SHE at pH 7, regardless of the identity of the protein. Protein film voltammetry of three different ferredoxins investigated in detail over a wide pH range shows that the novel species denoted as $[3Fe-4S]^{2-}$ is formed by a cooperative two-electron reduction of $[3Fe-4S]^0$ and there is a net uptake of three protons relative to the all-Fe(III) state $[3Fe-4S]^{1+}$. The protons are probably bound at or close to the cluster (accounting for the strong pH dependence and insensitivity to protein host), but H_2 is not evolved despite the negative potential at which $[3Fe-4S]^{2-}$ is formed. The hyper-reduced species which is produced reversibly in solution by four-electron electrochemical reduction of the 7Fe ferredoxin from *Sulfolobus acidocaldarius* contributes little absorbance in the visible spectral region, and shows an MCD spectrum with transitions below 400 nm that resemble features observed for Fe(II) rubredoxin. The EPR spectrum of the four-electron reduced protein differs significantly from that of the normal two-electron reduced form ($[3Fe-4S]^0$, $[4Fe-4S]^{1+}$); the signal at $g = 12$ assigned to $[3Fe-4S]^0$ disappears and changes occur to the spectrum in the $g = 1.94$ region which can be attributed to alterations in spin coupling with the $[4Fe-4S]^{1+}$ cluster. As an all-Fe(II) and (probably) protonated species performing *two-electron* redox reactions, $[3Fe-4S]^{2-}$ represents a fundamental entity of iron−sulfur cluster chemistry that has so far remained elusive. Structural and functional implications of this reactivity are considered.

Introduction

Iron−sulfur clusters are a ubiquitous class of protein active site and serve in a variety of biological functions including electron transfer, redox catalysis, reversible dehydration, and gene regulation.[1−3] Since these centers are capable of undergoing complex redox reactions, much attention has been directed at elucidating the factors that influence reduction potentials and determine the reactivities of clusters in different possible oxidation levels—chemistry that will also be relevant in considering their biological cycles of formation[4] and degradation. The best understood systems are the [2Fe−2S] and [4Fe−4S] clusters, with regard to which the following generalizations have evolved. First, the redox chemistry as exhibited in proteins is restricted to two adjacent oxidation levels.[5] Thus for [2Fe−2S] only the 2+/1+ couple is observed, whereas for [4Fe−4S] clusters, *either* the 2+/1+ *or* (more rarely) the 3+/2+ ("HiPIP") couple is utilized. Second, no stable cluster species formally composed only of Fe(II), i.e. $[2Fe-2S]^0$ or $[4Fe-4S]^0$, has been isolated and adequately characterized. Third, reduction potentials for Fe−S redox couples usually show little dependence on pH, thus indicating the absence of proton-transfer activity.

Against these ideas, several interesting observations have been made. First, it has become clear that higher nuclearity clusters ("superclusters") may readily exist in more than two oxidation states—examples being the so-called "P-cluster" ([8Fe−8S]) and Mo cofactor ([Mo7Fe−9S]) of nitrogenase,[6] and the "prismane" [6Fe−6S] cluster.[7] Furthermore, even for simple [2Fe−2S] and [4Fe−4S] clusters, the wider accessibility of more than two oxidation levels has been established by electrochemical experiments with synthetic analogues and indeed also with certain proteins; however, as expected, the reduction potentials of

[†] Inorganic Chemistry Laboratory.

[‡] University of East Anglia.

[⊗] Abstract published in *Advance ACS Abstracts,* August 15, 1996.

(1) Cammack, R. *Adv. Inorg. Chem.* **1992,** *38,* 281−322. Johnson M. K. *Encycl. Inorg. Chem.* **1994,** *4,* 1896−1915.

(2) Beinert, H.; Kennedy, M. C. *Eur. J. Biochem.* **1989,** *186,* 5−15. Kennedy, M. C.; Stout, C. D. *Adv. Inorg. Chem.* **1992,** *38,* 323−340. Flint, D. H.; Emptage, M. H.; Finnegan, M. G.; Fu, W.; Johnson M. K. *J. Biol. Chem.* **1993,** *268,* 14732−14742.

(3) Haile, D. J.; Rouault, T. A.; Harford, J. B.; Kennedy, M. C.; Blondin, G. A.; Beinert, H.; Klausner, R. D. *Proc. Natl. Acad. Sci. U.S.A.* **1992,** *89,* 11735−11739. Hidalgo, E.; Demple, B. *EMBO J.* **1994,** *13,* 138−146. Khoroshilova, N.; Beinert, H.; Kiley, P. J. *Proc. Natl. Acad. Sci. U.S.A.* **1995,** *92,* 2499−2503. Green, J.; Bennett, B.; Jordan, P.; Ralph, E. T.; Thomson, A. J.; Guest, J. R. *Biochem. J.* **1996,** *316,* 887−892.

(4) See, for example: Zheng, L.; Dean, D. R. *J. Biol. Chem.* **1994,** *269,* 18723−18726.

(5) Carter, C. W. In *Iron−Sulfur Proteins*; Lovenberg, W., Ed.; Academic Press Inc.: New York, NY, 1977; Vol. 3.

(6) Smith, B. E.; Eady, R. R. *Eur. J. Biochem.* **1992,** *205,* 1−15.

(7) Pierik, A. J.; Hagen, W. R.; Dunham, W. R.; Sands, R. H. *Eur. J. Biochem.* **1992,** *206,* 705−719.

S0002-7863(96)01465-5 CCC: $12.00

adjacent redox couples are widely separated.[8−10] Second, there have been several reports of generation of all-Fe(II) clusters using strong reductants or electrochemical methods. These include the Rieske [2Fe−2S] center of complex III[9] and the [2Fe−2S] center in *Anabaena variabilis* ferredoxin,[11] although in no case so far have products been subjected to extensive spectroscopic characterization. From respective EPR and Mössbauer studies on *Azotobacter vinelandii* nitrogenase proteins, it has been proposed that a $[4Fe-4S]^0$ cluster can be attained in the Fe protein,[12] and that the most highly reduced level of the P-cluster of the MoFe protein corresponds to an all-Fe(II) state.[13] Third, there have been isolated reports of protonation accompanying electron transfer at 2Fe and 4Fe centers, including non-protein analogues, ferredoxins, and the Rieske [2Fe−2S] cluster from complex III.[14−18]

Throughout recent electrochemical studies it has been noted that [3Fe−4S] clusters exhibit redox chemistry that is strikingly different from the other simple clusters. Most importantly the "0" level, which is regarded as the normal "reduced" form, undergoes facile and reversible uptake of a further *two electrons*.[19−23] This reaction has been observed for all [3Fe−4S]-cluster-containing proteins so far examined, i.e. the 7Fe ferredoxins from *Desulfovibrio africanus* (Fd III),[19,20] *Azotobacter vinelandii* (Fd I),[21] and *Sulfolobus acidocaldarius*.[22] Experiments have also suggested that the reaction occurs in fumarate reductase,[24] and researchers have reported similar observations of further reduction of the $[3Fe-4S]^0$ cluster in studies of the 3Fe ferredoxins from *Desulfovibrio gigas* (Fd II)[25] and *Pyrococcus furiosus*,[26] beef heart aconitase,[27] and a previous study of the 7Fe ferredoxin from *Sulfolobus* sp7.[28] We have postulated[22] that one factor distinguishing [3Fe−4S] clusters from other low-nuclearity clusters may be an intrinsic ability for protonation. This has been inferred from extensive studies on the [3Fe−4S] cluster of *Azotobacter* (*chroococcum* and *vinelandii*) Fd I[21,29−34] and recently also for the [3Fe−4S] cluster of *Sulfolobus acidocaldarius* ferredoxin.[22] Protonation assists electronation by enabling multiple sequential redox processes to occur without accumulating negative charge.[35] Although studies with non-protein model systems have indicated that [4Fe−4S] clusters can bind protons,[14−16] almost all protein-bound clusters that have been examined in sufficient detail show only a weak interaction with protons[17] at least as evidenced from the lack of significant changes in reduction potential with pH. By contrast, the open-faced structure of [3Fe−4S] with its "crown" of three μ_2-S atoms may provide an effective site (or sites) for protonation. This is certainly supported (at least indirectly) by the fact that in some proteins the [3Fe−4S] cluster exhibits *Lewis basicity* by coordinating a fourth metal ion. This reactivity has been established for mitochondrial aconitase,[36] *Desulfovibrio africanus* Fd III,[20,37] *Desulfovibrio gigas* Fd II,[25,38] *Pyrococcus furiosus* Fd,[39] and most recently for a non-protein cluster analogue $[Fe_3S_4(LS_3)]^{3-}$ (LS_3 = a tripodal ligand).[40,41] A further point of interest is how clusters containing Fe exclusively in the 2+ oxidation state can be stabilized. High-spin iron(II) is low in the Irving−Williams series and is not expected to form strong complexes in proteins unless bound within a specialized structure such as a porphyrin or induced to become low spin.[42]

In this paper, we have collated electrochemical results for several ferredoxins and describe spectroscopic studies on the "hyper-reduced" $[3Fe-4S]^{2-}$ cluster generated in the ferredoxin from *Sulfolobus acidocaldarius*. We have determined that formation of $[3Fe-4S]^{2-}$ is reversible and, in the weakly acidic/neutral region of pH, consumes a total of three protons for the overall three-electron reduction of $[3Fe-4S]^{1+}$. Spectroscopic properties are measured, and structural and functional properties of the novel product are considered.

(8) Henderson, R. A.; Sykes, A. G. *Inorg. Chem.* **1980,** *19,* 3103−3105.
(9) Verhagen, M. F. J. M.; Link, T. A.; Hagen, W. R. *FEBS Lett.* **1995**, *361,* 75−78.
(10) Heering, H. A.; Bulsink, Y. B. M.; Hagen, W. R.; Meyer, T. E. *Eur. J. Biochem.* **1995,** *232,* 811−817.
(11) Im, S.-C.; Lam, K.-Y.; Lim, M.-C.; Ooi, B.-L.; Sykes, A. G. *J. Am. Chem. Soc.* **1995**, *117,* 3635−3636.
(12) Watt, G. D.; Reddy, N. F. R. *J. Inorg. Biochem.* **1994**, *53*, 281−294.
(13) Smith B. E. In *Nitrogen Fixation: The Chemical-Biochemical Genetic Interface*; Müller, A., Newton, W. E., Eds.; Plenum Press: New York, London, 1983; pp 23−62.
(14) Tsai, H.; Sweeney, W. V.; Coyle C. L. *Inorg. Chem.* **1985,** *24,* 2796−2798.
(15) Henderson, R. A.; Oglieve, K. E. *J. Chem. Soc., Chem. Commun.* **1994,** 377−379.
(16) Nakamoto, M.; Tanaka, K.; Tanaka, T. *Bull. Chem. Soc. Jpn.* **1988,** *61,* 4099−4105.
(17) Magloizzo, R. S.; McIntosh, B. A.; Sweeney, W. V. *J. Biol. Chem.* **1982,** *257,* 3506−3509.
(18) Link, T. A.; Hagen, W. R.; Pierik, A. J.; von Jagow, G. *Eur. J. Biochem.* **1992**, *208*, 685−691.
(19) Armstrong, F. A.; Butt, J. N.; George, S. J.; Hatchikan, E. C.; Thomson, A. J. *FEBS Lett.* **1989,** *259,* 15−18.
(20) Butt, J. N.; Armstrong, F. A.; Breton, J.; George, S. J.; Thomson, A. J.; Hatchikian, E. C. *J. Am. Chem. Soc.* **1991,** *113,* 6663−6670.
(21) Shen B.; Martin, L. L.; Butt, J. N.; Armstrong, F. A.; Stout, C. D.; Jensen, G. M.; Stephens, P. J.; La Mar, G. N.; Gorst, C. M.; Burgess, B. K. *J. Biol. Chem.* **1993,** *268,* 25928−25939.
(22) Breton, J. L.; Duff, J. L. C.; Butt, J. N.; Armstrong, F. A.; George, S. J.; Pétillot, Y.; Forest, E.; Schäfer, G.; Thomson, A. J. *Eur. J. Biochem.* **1995,** *233,* 937−946.
(23) Armstrong, F. A. *Adv. Inorg. Chem.* **1992,** *38,* 117−163.
(24) Sucheta, A.; Cammack, R.; Weiner, J.; Armstrong, F. A. *Biochemistry* **1993,** *32,* 5455−5465.
(25) Moreno, C.; Macedo, A. L.; Moura, I.; LeGall, J.; Moura, J. J. G. *J. Inorg. Biochem.* **1994**, *53,* 219−234.
(26) Smith, E. T.; Blamey, J. M.; Zhou, Z. H.; Adams, M. W. W. *Biochemistry* **1995**, *34*, 7161−7169.
(27) Tong, J.; Feinberg, B. A. *J. Biol. Chem*. **1994,** *269*, 24920−24927.
(28) Iwasaki, T.; Wakagi, T.; Isogai, Y.; Tanaka, K.; Iizuka, T.; Oshima, T. *J. Biol. Chem.* **1994**, *269*, 29444−29450.
(29) George, S. J.; Richards, A. J. M.; Thomson, A. J.; Yates, M. G. *Biochem. J.* **1984,** *224,* 247−251.
(30) Armstrong, F. A.; George, S. J.; Thomson, A. J.; Yates, M. G. *FEBS Lett.* **1988,** *234,* 107−110.
(31) Iismaa, S. E.; Vázquez, A. E.; Jensen, G. M.; Stephens, P. J.; Butt, J. N.; Armstrong, F. A.; Burgess, B. K. *J. Biol. Chem.* **1991,** *266,* 21563−21571.
(32) Johnson, M. K.; Bennett, D. E.; Fee, J. A.; Sweeney, W. V. *Biochim. Biophys. Acta* **1987,** *911,* 81−94.
(33) Butt, J. N.; Sucheta, A.; Martin, L. L.; Shen, B.; Burgess, B. K.; Armstrong, F.A. *J. Am. Chem. Soc.* **1993,** *115,* 12587−12588.
(34) (a) Hu, Z.; Jollie, D.; Burgess, B. K.; Stephens, P. J.; Münck, E. *Biochemistry* **1994**, *33*, 14475−14485. (b) Stout, C. D. *J. Biol. Chem.* **1993,** *268*, 25920−25927.
(35) See for example: Sellman, D.; Mahr, G.; Knoch, F.; Moll, M. *Inorg. Chim. Acta* **1994,** *224*, 45−59. Mitchell, R.; Rich, P. R. *Biochim. Biophys. Acta* **1994,** *1186*, 19−26.
(36) Beinert, H.; Kennedy, M. C. *Eur. J. Biochem.* **1989,** *186,* 5−15.
(37) Butt, J. N.; Sucheta, A.; Armstrong, F. A.; Breton, J.; Thomson, A. J.; Hatchikian, E. C. *J. Am. Chem. Soc.* **1991,** *115,* 8948−8950. Butt, J. N.; Niles, J.; Armstrong, F. A.; Breton, J.; Thomson, A. J. *Nature Struct. Biol.* **1994,** *1,* 427−433. Butt, J. N.; Breton, J.; Thomson, A. J.; Armstrong, F. A. Submitted for publication.
(38) Surerus, K. K.; Münck, E.; Moura, I.; Moura, J. J. G.; LeGall, J. *J. Am. Chem. Soc.* **1987,** *109*, 3805−3806. Moura, I.; Moura J. J. G.; Münck, E.; Papaefthymiou, V.; LeGall, J. *J. Am. Chem. Soc.* **1986,** *108*, 349−351.
(39) Finnegan, M. G.; Conover, R. C.; Park, J-B.; Zhou, Z. H.; Adams, M. W. W.; Johnson, M. K. *Inorg. Chem.* **1995,** *34,* 5358−5369. Fu, W. G.; Telser, J.; Hoffman, B. M., Smith E. T.; Adams, M. W. W.; Finnegan, M. G.; Conover, R. C.; Johnson, M. K. *J. Am. Chem. Soc.* **1994,** *116*, 5722−5729. Srivastava, K. K. P.; Surerus, K. K.; Conover, R. C.; Johnson, M. K.; Park, J.-B.; Adams, M. W. W.; Münck, E. *Inorg. Chem.* **1993,** *32*, 927−936.
(40) Zhou, J.; Holm, R. H. *J. Am. Chem. Soc.* **1995,** *117,* 11353−11354.
(41) Zhou, J.; Hu, Z.; Münck, E.; Holm, R. H. *J. Am. Chem. Soc.* **1996,** *118,* 1966−1980.
(42) da Silva, J. R. R. F.; Williams, R. J. P. In *The Biological Chemistry of the Elements: The Inorganic Chemistry of Life*; Oxford University Press: New York, 1991.

Methods

Ferredoxins. The 7Fe ferredoxin (Fd III) from *Desulfovibrio africanus* (Strain Benghazi), prepared as described in the literature, was supplied by Dr E. C. Hatchikian, as were samples of the 4Fe ferredoxins (Fd I and Fd II) from the same organism.[43] Cells of *Sulfolobus acidocaldarius* (strain DSM 639) were provided by Drs. N. Raven and R. Sharp (Centre for Applied Microbiology and Research, Porton Down, U.K.), and the 7Fe ferredoxin was isolated as described previously.[22] Samples of *Azotobacter vinelandii* Fd I were provided by Professor Barbara Burgess. Final concentrations were determined using published extinction coefficients (ϵ/ mM^{-1} cm^{-1}, λ/ nm) of 29.0, 408 (*Sulfolobus acidocaldarius*),[44] 28.6, 408 (*Desulfovibrio africanus*),[45] and 29.8, 400 (*Azotobacter vinelandii*).[46]

Electrochemistry. Purified water of resistivity ~18 MΩ·m (Millipore) was used in all experiments. Reagents were purchased from Aldrich or BDH and were of at least analytical grade. The buffers Mes, Hepes, and Taps and co-adsorbates neomycin sulfate and polymyxin B sulfate were purchased from Sigma. Neomycin and polymyxin solutions were prepared as concentrated stocks (0.2 M and 15 mM (i.e. 20 mg/mL), respectively) and adjusted to pH 7.4.

Analog DC cyclic voltammetry and bulk electrolysis were carried out with an Ursar Instruments potentiostat, and voltammograms and bulk electrolytic current−time traces were recorded with Kipp and Zonen XY and YT recorders, respectively. The all-glass cell and three-electrode system used for protein film voltammetry and much of the bulk solution voltammetry have been described previously.[22,31,47] The saturated calomel reference electrode (SCE) was held at 22 °C at which we have adopted E(SCE) = +243 mV versus the Standard Hydrogen Electrode (SHE): all values were adjusted to the SHE scale. The sample compartment was maintained at 0 °C. The pyrolytic graphite "edge" (PGE) electrode (surface area typically 0.18 cm^2) was polished before experiments with an aqueous alumina slurry (Buehler Micropolish:0.3 μm for solution electrochemistry or 1.0 μm for protein film voltammetry) and then sonicated extensively to remove traces of Al_2O_3.

A graphite pot was used as an electrode to prepare solutions for spectroscopic studies. This consisted of a cylindrical block of pyrolytic graphite, bored out to give a hole (1 cm in diameter) such that the inside walls were "edge" surface, and cemented to a graphite base (using insulating epoxy) such that it also projected "edge" surface into the pot. The walls and base were wired separately. The pot was raised into a glass circulating jacket which was part of an all-glass cell with ports receiving reference (SCE, Luggin capillary junction) and auxillary (Pt, salt-bridge "Vycor" junction) side arms each dipping into the sample solution. The entire cell was set up in an anaerobic glovebox (Belle Technology, Poole, U.K.) with an inert atmosphere of N_2 (O_2 < 0.5 ppm), fresh charges of catalyst being used for each run. For cyclic voltammetry, only the base was connected. For bulk electrolysis, all parts of the electrode were used and the solution was stirred by magnetic micro-flea. The high-surface-area PGE cell gave reduction half-times of ca. 2 min for a 80 μM solution, 200 μL in volume.

For all electrochemical studies, ferredoxin solutions were prepared by thawing frozen pellets of concentrated protein stock solution into the required buffer solutions at 4 °C and dialyzing in an Amicon 8MC unit equipped with a microvolume assembly and a YM3 membrane. For protein film experiments, the ferredoxin solution used to coat the electrode contained 0.1 M NaCl, 20 mM Hepes, and polymyxin (typically 200 μg/mL) or in some cases neomycin (2 mM). The pH of this solution was adjusted to 7.0 at 0 °C. The buffer−electrolyte solution in the electrochemical cell consisted of 0.1 M NaCl and a mixed buffer system (5 mM in each of acetate, Mes, Hepes, and Taps) at 0 °C. The freshly polished electrode surface was painted with ca. 1 μL of chilled protein solution from a fine capillary and then placed promptly into the cell solution. To stabilize protein films, the cell solution also contained 200 μg/mL of polymyxin or 2 mM neomycin. The pH of this solution was checked after each set of experiments, with the pH electrode calibrated at 0 °C. For bulk solution voltammetry and controlled potential bulk electrolysis, ferredoxin solutions contained 0.1 M NaCl with 20 mM Hepes or 20 mM Mes. Small aliquots of neomycin stock solution were added (final concentration 1.0−2.0 mM) in order to promote a strong and persistent electrochemical response. Reduction potentials were calculated as the average of the anodic and cathodic peak potentials, $E^{o\prime} = {}^1/_2(E_{pa} + E_{pc})$, and could be determined for couple C′ even where signals overlayed those of couple B′ (see results). This was due to the much sharper form of C′ compared with B′, since 2-electron signals theoretically have four times the height and half the width of 1-electron signals.[47]

Spectroscopy. Perpendicular-mode EPR spectroscopy was performed on an X-band (9.44 GHz) Bruker ER200-D SRC spectrometer equipped with an Oxford Instruments ESR-900 He-flow cryostat and a TE102 cavity. Parallel-mode spectra were obtained using a Bruker dual-mode cavity (perpendicular-mode: 9.60 GHz; parallel-mode: 9.40 GHz). The microwave frequency was measured with a Marconi 2440 counter. Spin densities were estimated from integration of EPR absorption spectra by comparison with a 1 mM Cu(II)−EDTA standard.[48]

Low-temperature MCD measurements were made using a Jasco J-500D dichrograph and an Oxford Instruments split-coil superconducting magnet SM-4. Procedures for measuring MCD spectra have been described elsewhere.[49] Protein samples were prepared by anaerobic bulk electrolysis at the required potentials in the cell described above. After electrolysis, the aqueous sample (containing up to 280 μM ferredoxin) was diluted with ethylene glycol to 50% (v/v) and the potential was reapplied to ensure complete reduction. The sample was then divided and transferred by syringe to a 1 mm pathlength MCD cell and to an EPR tube.

UV−visible absorption spectra of ferredoxin solutions electrolyzed at various potentials were measured using a spectrometer cell-block located in the glovebox and linked by fibre-optic cables to a MG-6000 diode-array spectrometer unit (Hi-Tech Scientific, Salisbury, England). Samples were transferred between the electrochemical cell and the cuvette by syringe, with less than 10% re-oxidation estimated to be occurring in the process.

Results

Electrochemistry. 1. Film Voltammetry. Figure 1 shows film voltammograms of *A. vinelandii* Fd I, *D. africanus* Fd III, and *S. acidocaldarius* Fd. In each case, three couples are observed, denoted A′, B′, and C′ (the "prime" indicating that they refer to experiments in which the sample is adsorbed as a film, as opposed to being present in bulk solution[19]). Couples A′ and B′ correspond to the established redox processes [3Fe−4S]$^{1+/0}$ and [4Fe−4S]$^{2+/1+}$, respectively;[19−23] however, for all three proteins, the voltammogram is dominated by couple C′ which is observed in the region of −700 mV. Similar observations of this extra redox couple have been reported for other proteins containing [3Fe−4S] clusters.[24−28] Furthermore, in the case of *Da* Fd III, a definitive link with the [3Fe−4S] cluster was established by correlating the disappearance of couple C′ with the transformation of [3Fe−4S]^0 into various cubane-type adducts [M3Fe−4S]$^{2+}$.[19,20] That this reaction occurs at the [3Fe−4S] cluster as opposed to residues on the peptide chain (e.g. disulfide bridges) is supported by the fact that *Da* Fd III[50] and *Sa* Fd[51] each contain just seven cysteines, all of which are implicated in cluster binding.[52]

For *Da* Fd III,[19] *Sa* Fd[22] (pH >7), and *Av* Fd I (pH >8) the ratios of areas C′/A′ measured either from reduction or oxidation waves were determined to be 2.0 ± 0.3, while for *Av* Fd I (pH <8) and *Sa* Fd (pH <7), where C′ tends to overlap with B′, the

(43) Hatchikian, E. C.; Bruschi, M. *Biochim. Biophys. Acta* **1981,** *634,* 41−51.
(44) Kerscher, L.; Nowitzki, S.; Oesterhelt, D. *Eur. J. Biochem.* **1982,** *128,* 223−230.
(45) Bovier-Lapierre, G.; Bruschi, M.; Bonicel, J.; Hatchikian, E. C. *Biochim. Biophys. Acta* **1987,** *918,* 20−26.
(46) Stephens, P. J.; Jensen, G. M.; Devlin, F. J.; Morgan, T. V.; Stout, C. D.; Martin, A. E.; Burgess, B. K. *Biochemistry* **1991,** *30,* 3200−3209.
(47) Armstrong, F. A.; Butt, J. N.; Sucheta, A. *Meth. Enzymol.* **1993,** *227,* 479−500.
(48) Aasa, R.; Vänngård, T. *J. Magn. Reson.* **1975**, *19,* 308−315.
(49) Thomson, A. J.; Cheesman, M. R.; George, S. J. *Meth. Enzymol.* **1993**, *226,* 199−231.

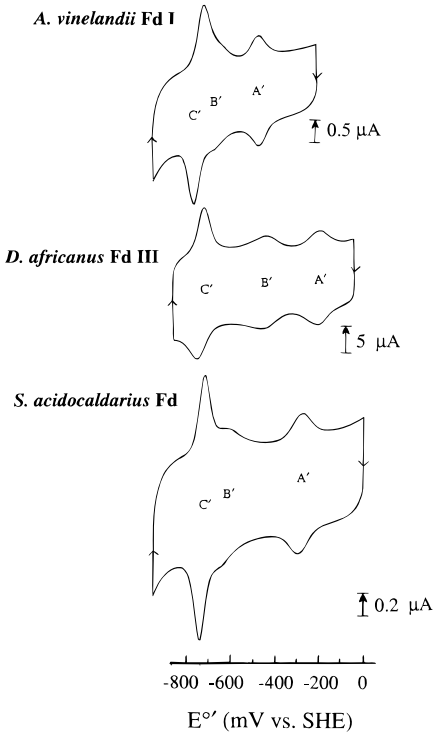

Figure 1. Film voltammograms of *A. vinelandii* Fd I, *D. africanus* Fd III, and *S. acidocaldarius* Fd at 0 °C. Conditions: *A.v.* Fd I, 100 μM in 20 mM Hepes, 0.1 M NaCl, pH 7.0, co-adsorbate 200 μg/mL polymyxin, scan rate 20 mVs^{-1}; *D.a.* Fd III, 100 μM in 20 mM Hepes, 0.1 M NaCl, pH 7.0, co-adsorbate 2 mM neomycin, scan rate 191 mV s^{-1}; *S.a.* Fd, 100 μM in 20 mM mixed buffer, 0.1 M NaCl, pH 7.3, co-adsorbate 200 μg/mL of polymyxin, scan rate 10 mV s^{-1}.

ratio (B′ + C′)/A′ was 3.0 ± 0.3.[53] The narrow half-height widths (≤60 mV) of the C′ couple reduction and oxidation waves obtained at slow scan rates show that the two electrons are transferred cooperatively (i.e. that the reduction potential for the couple [3Fe−4S]$^{0/1-}$ is similar to or more negative than for [3Fe−4S]$^{1-/2-}$). We shall refer to the states [3Fe−4S]$^{1-}$ and [3Fe−4S]$^{2-}$ as "super-reduced" and "hyper-reduced", respectively. The appearance of couple C′ in each case depended markedly upon pH in that use of higher pH (e.g. above 8 for *Av* Fd I) gave broadened waves of diminished amplitude. Similar results were obtained for the 7Fe ferredoxins from *Azotobacter chroococcum*[30] and *Thermoplasma acidophilum*[54] and the 3Fe ferredoxin from *Pyrococcus furiosus*.[54]

As shown in Figure 2, reduction potentials of the redox couples assigned to the 3Fe cluster (A′ and C′) are dependent on pH. By contrast, reduction potentials of couple B′ show much less dependence on pH in each case. Data were fitted either to eq 1 (where just one pK is evident for the reduced species) or to eq 2 (where pK values are evident for both oxidized and reduced species).[55]

$$E^{\circ\prime} = E^{\circ\prime}_{\mathrm{alk}} + \frac{RT}{nF}\ln\left[1 + \frac{(a_{\mathrm{H}^+})^y}{K_{\mathrm{red}}}\right] \qquad (1)$$

For eq 1, $E^{\circ\prime}_{\mathrm{alk}}$ is the reduction potential in the limit of high pH, a_{H^+} is the H^+ activity, n is the number of electrons transferred, y is the number of protons transferred, and K_{red} is the apparent H^+-dissociation constant for the reduced species ([3Fe−4S]^0 or [3Fe−4S]$^{2-}$ as appropriate). The terms R, T, and F have their usual meanings.

$$E^{\circ\prime} = E^{\circ\prime}_{\mathrm{m}} + \frac{RT}{nF}\ln\left[\frac{(a_{\mathrm{H}^+})^3 + (a_{\mathrm{H}^+})^2 K_{\mathrm{red}}}{a_{\mathrm{H}^+} + K_{\mathrm{ox}}}\right] \qquad (2)$$

For eq 2, K_{red} is the apparent H^+-dissociation constant for [3Fe−4S]$^{2-}$, K_{ox} is the H^+-dissociation constant for [3Fe−4S]^0, $E^{\circ\prime}_{\mathrm{m}}$ is the reduction potential at pH 0, and other terms are as defined for eq 1. The n-values for couples A′ and C′ were fixed at 1.0 and 2.0, respectively, since these quantities had been determined experimentally as described above. The results of studies of the pH dependence of couples A′ and C′ are shown in Table 1 and summarized in Table 2. From these data and examination of Figure 2, several features are noted.

First, considering couple A′, a pH dependence of $E^{\circ\prime}$ with a well-defined pK_{red} has previously been established for *Sa* Fd,[22] for *Av* (and *Ac*) Fd's I,[21,30] and for a mutant form (D15N) of *Av* Fd I in which an aspartate residue adjacent to the [3Fe−4S] cluster is replaced by asparagine.[21] The pK_{red} values observed (respectively 5.8, 7.8, and 6.9) have been proposed to correspond to single protonation of the one-electron reduced [3Fe−4S]^0 cluster, although the exact location of the proton has not been determined conclusively.[34] Below respective pK_{red} values, the slope d$E^{\circ\prime}$/d(pH) is −54.2 mV, consistent with a transfer ratio H^+/e^- = 1.0 (0 °C). The corresponding graph for *Da* Fd III suggests a much lower pK_{red} value (4.9) for couple A′, and the slope does not attain the value expected for H^+/e^- = 1.[56]

Second, for couple C′, the pH dependences of $E^{\circ\prime}$ again suggest protonation equilibria. The situation is clearly much more complicated at higher pH since couple C′ becomes less observable as the pH is increased: in each case the pH dependence of $E^{\circ\prime}$ appears to reflect this feature, since the slopes diminish above pH 8. We therefore focus our attention on the data obtained for the neutral/weakly acidic pH region in which the voltammetric waves of the C′ couple have the size and form expected for a clean two-electron reaction. The simplest behavior is shown by *Av* Fd I where the slope below pH 8 is consistent with a transfer ratio H^+/e^- = 1.0, implying a concomitant uptake of $2H^+$ and $2e^-$ by the [3Fe−4S]^0 cluster which (below the pK_{red} of 7.8) has one proton already bound. The data for *Sa* Fd and *Da* Fd III can be fitted to eq 2[55] which describes transfer of 1.0 H^+/e^- and 1.5 H^+/e^- above and below respective pK_{ox} values of 6.3 and 4.7. (Transfer ratios of 1.0 and 1.5 for couple C′ correspond to uptakes of $2H^+$ per $2e^-$ and $3H^+$ per $2e^-$, respectively.) Again, breaks apparent at higher pH (pK_{red} = 7.0 and 6.5) coincide approximately with the onset of wave attenuation.

The complex forms of the pH dependences of $E^{\circ\prime}$ values for A′ and (particularly) C′ are difficult to define precisely. A more

(50) Bovier-Lapierre, G.; Bruschi, M.; Bonicel, J.; Hatchikian, E. C. *Biochim. Biophys. Acta* **1987,** *913,* 20−26.

(51) Minami, Y.; Wakabayashi, S.; Wada, K.; Matsubara, H.; Kerscher, L.; Oesterhelt, D. *J. Biol. Chem. (Tokyo)* **1985,** *97,* 745−753.

(52) Couple C′ is observed in similar manner in the C24A mutant of *Av* Fd I, which has just one additional cysteine (C11) and therefore can have no internal disulfide bridges which could have provided possible sites for the further reduction. See: Iismaa, S. E.; Vasquez, A. E.; Jensen, G. M.; Stephens, P. J.; Butt, J. N.; Armstrong, F. A.; Burgess, B. K. *J. Biol. Chem.* **1991,** *266,* 21563−21571.

(53) At pH <5, couples B′ and C′ overlapped also for *Da* Fd III. Analysis of the combined envelope gave a ratio (B′ + C′)/A′ = 3.0 ± 0.3. Where overlap was marginal, the problem was minimized by use of a low scan rate.

(54) Fawcett, S. E. J., Davis, D., Breton, J. L. J.; Thomson, A. J.; Armstrong, F. A. In preparation.

(55) Clark, W. M. In *Oxidation-reduction Potentials of Organic Systems*; Williams and Wilkins: Baltimore, 1960.

(56) The lower gradient obtained for Fd III may be a result of competing ionizations (such as a pK_{ox}) occurring at a slightly lower pH value. Fd III contains an ionizable aspartate residue that may coordinate the metal ion (M) incorporated upon transformation of the [3Fe−4S] cluster into [M3Fe−4S]. See refs 20 and 37.

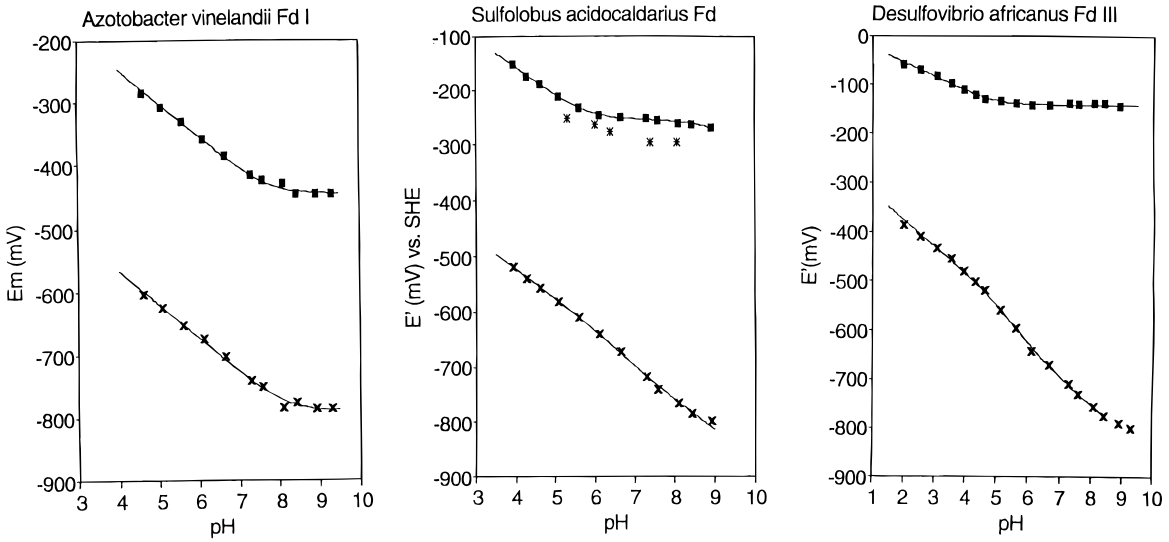

Figure 2. Plots of $E^{\circ\prime}$ versus pH for A′ (■) and C′ (×) couples of *A. vinelandii* Fd I, *D. africanus* Fd III, and *S. acidocaldarius* Fd. (*) Values in bulk solution measured for *S. acidocaldarius* Fd. Temperature 0 °C.

Table 1. Reduction Potentials at 0 °C (mV versus SHE)

	A. vinelandii Fd I		*S. acidocaldarius* Fd		*D. africanus* Fd III	
pH	C′	A′	C′	A′	C′	A′
2.0					−385.5	−58.0
2.5					−409.5	−70.0
3.1					−432.0	−83.0
3.5					−455.5	−98.0
3.9			−519.0	−153.0	−480.5	−110.5
4.3			−539.5	−175.5	−501.5	−122.0
4.6	−604.0	−284.0	−557.0	−188.0	−518.0	−129.0
5.1	−625.5	−308.0	−582.0	−210.5	−558.0	−134.5
5.6	−652.5	−331.0	−610.5	−233.0	−595.0	−138.0
6.1	−675.0	−358.0	−640.5	−245.0	−642.0	−143.0
6.6	−703.0	−385.5	−673.0	−250.5	−670.0	−142.0
7.3	−740.5	−415.5	−718.0	−250.5	−710.0	−140.0
7.6	−750.5	−423.0	−740.5	−255.5	−730.0	−141.0
8.1	−784.0	−428.0	−766.5	−260.5	−756.5	−138.0
8.4	−775.5	−446.5	−785.5	−263.0	−775.5	−140.0
8.9	−786.0	−446.5	−798.0	−268.0	−789.0	−145.5
9.3	−785.5	−445.5			−799.5	

Table 2

	couple A′: $[3Fe-4S]^{1+/0}$		couple C′: $[3Fe-4S]^{0/2-}$		couples (A′ + C′): $[3Fe-4S]^{1+/2-}$	
ferredoxin	$dE^{\circ\prime}/dpH$[a]	$pK_{red(A')}$	pK_{ox}	$pK_{red(C')}$	$(dE^{\circ\prime}/dpH)_{av}$[b]	total H^+/e^-
A. vinelandii Fd I	−54.2	7.7		8.1	−50.1	0.92
S. acidocaldarius Fd	−54.2	5.8	6.3	7.0	−49.8	0.92
D. africanus Fd III	−29.5	4.9	4.7	6.5	−51.4	0.95

[a] Units: mV per pH unit. [b] $(dE^{\circ\prime}/dpH)_{av} = (dE/dpH)\ \{^1/_3[A'_i + 2C'_i)]\}$ calculated for all individual data points A'_i and C'_i below $pK_{red(C')}$.

satisfactory picture of the *overall* proton uptake of the A′ and C′ couples in the neutral/weakly acidic region is afforded by analyzing the total H^+/e^- ratio, i.e. by averaging the $n\ E^{\circ\prime}$ values for A′ and C′ to give values of $(dE^{\circ\prime}/dpH)_{av}$. In this way, we found for each protein (Table 2) that the net ratio H^+/e^- is close to 1.0, i.e. that there is an *overall uptake* of *three* protons in the 3-electron reduction of $[3Fe-4S]^{1+}$ to $[3Fe-4S]^{2-}$.

The proposed sequence of electron-transfer reactions is depicted in Scheme 1. The less well-defined situation for *Da* Fd III reflects the much lower pK_{red} for couple A' and uncertainty about whether this is due to protonation of $[3Fe-4S]^0$.[56] The picture that emerges is that formation of the species $[3Fe-4S]^{2-}$ depends upon the uptake of three protons; indeed,

Scheme 1

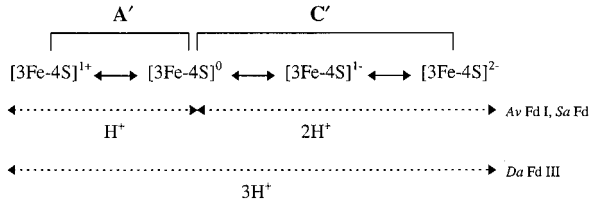

formation of $[3Fe-4S]^{2-}$ does not proceed readily under more alkaline conditions. In the neutral/weakly acidic region of pH, voltammograms for each protein show well-defined waves for couple C′, integration of which clearly reveals a 2-electron reaction. Broadly speaking, in this pH region, proton uptake appears apportioned between the two redox couples A′ and C′ in a mutually compensating manner (*i.e.* pK_{ox} values for couple C′ coincide approximately with pK_{red} for couple A′). That the protons involved are not reduced to H_2, despite the very negative potential, is apparent from the shape of the oxidation wave of couple C′ and its size relative to that of the reduction wave, each of which are as expected for a non-catalytic process even at low scan rates.

2. Solution Voltammetry and Bulk Electrolysis. Experiments carried out with solutions of *Av* Fd I or *Da* Fd III have consistently shown that couple C (by contrast with couples A and B) is limited to molecules that are adsorbed on the electrode surface.[19,57] This restriction may arise from kinetic complications in synchronizing multiple, sequential proton−electron transfer reactions.[58] The important observation now made is that this restriction appears to be relaxed for *Sa* Fd, and provides the opportunity to generate the products of couple C in solution form for closer examination. Possibly related to this is the observation that both reduction and oxidation waves of couple

(57) Armstrong, F. A.; George, S. J.; Cammack, R.; Hatchikian, E. C.; Thomson, A. J. *Biochem. J.* **1989,** *264,* 265−273.

(58) In recent studies of reversible (non-catalytic) and associated catalytic electrochemistry of several enzymes, including succinate dehydrogenase, fumarate reductase, and cytochrome *c* peroxidase, we have linked the electrocatalytic behavior to adsorbed rather than freely diffusing enzyme molecules. Organization of a compact protein assembly at the electrode surface may be crucial for efficient, *multiple*, and coupled electron exchange, as required in catalytic processes or in complex multielectron/multiproton reactions. See ref 22, and the following: Sucheta, A.; Ackrell, B. A. C.; Cochran, B.; Armstrong, F. A. *Nature* **1992,** *356,* 361−362. Mondal, M. S.; Fuller, H. A.; Armstrong, F. A. *J. Am. Chem. Soc.* **1996,** *118,* 263−264. Hirst, J.; Sucheta, A.; Ackrell, B. A. C.; Armstrong, F. A. *J. Am. Chem. Soc.* **1996**, *118,* 5031−5038.

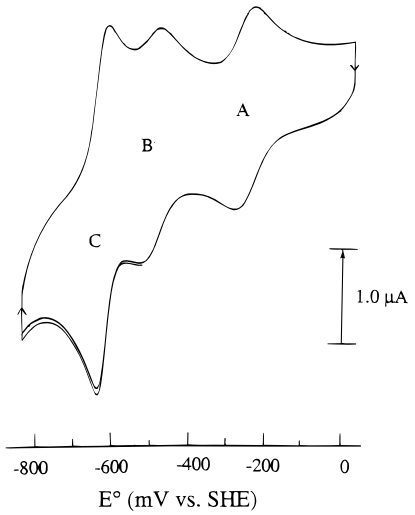

Figure 3. Bulk solution cyclic voltammogram of 80 μM *S. acidocaldarius* ferredoxin in 20 mM Mes, 0.1 M NaCl, 0.1 mM EGTA, pH 6.4, co-adsorbate 2 mM neomycin, scan rate 5 mV s^{-1}, temperature 0 °C.

C′ appear somewhat sharper (suggesting that any coupled chemical steps are faster) for *Sa* Fd than for the other ferredoxins studied under comparable conditions of pH and scan rate. A cyclic voltammogram obtained for a solution of *Sa* Fd is shown in Figure 3. Each of the redox couples (A, B, *and* C) behaves as expected for a diffusion-controlled electrode reaction, i.e. peak currents (i_p) are directly proportional to the square root of scan rate ($\nu^{1/2}$) for $\nu \leq 20$ mV s^{-1},[59] and the waves collapse to a sigmoidal form when the electrode is rotated (600 rpm, scan rate $\leq$10 mV s^{-1}). Results for the limited pH range studied in bulk solution are included in the graph in Figure 2, where it can be seen that the $E^{\circ\prime}$ values are more negative than obtained for films, but only by approximately 20 mV. It was thus feasible to use direct electrochemical methods to generate samples of the protein containing the three-electron reduced [3Fe−4S] cluster for investigation by EPR, UV/visible, and MCD spectroscopy.

Samples of *Sulfolobus acidocaldarius* Fd were subjected to coulometrically-monitored electrolysis at various applied potentials. For predictions of best end points and for analysis of titration data, it was necessary to consider the complications posed by the close proximity of couples B and C in order to select optimized potentials at which to electrolyze. Nernst plots were constructed using the reduction potentials determined by solution voltammetry in order both to predict the total number of electron equivalents consumed for a given potential and to determine the potentials required to achieve optimal resolution of species at each stage. Figure 4 shows the calculated profile for pH 6.4, together with actual results obtained.

The electrolyses showed several important features. First, as expected, well-defined quantitative relationships were observed when comparing electrolyses carried out at potentials corresponding to different end points of the Nernst plots. To correct for uncertainties in the actual amount of sample undergoing electrolysis, data were also normalized with respect to the well-established, one-electron $[3Fe-4S]^{1+/0}$ redox transition. In this way, for example, it was ascertained that at pH 6.4, the number of electron equivalents required for exhaustive reduction of solutions at very negative potentials (i.e. −870 mV) is *four times* that required at −457 mV, and *twice* that for electrolysis at potentials between −594 and −612 mV. Second,

(59) Bard, A. J.; Faulkner, L. R. In *Electrochemical Methods; Fundamentals and Applications*; Wiley: New York, 1980.

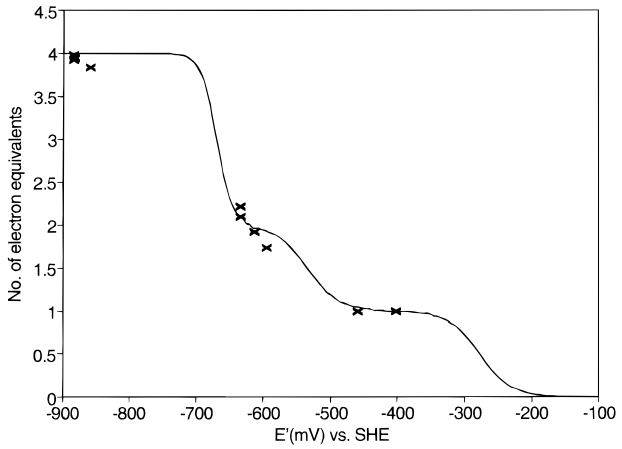

Figure 4. "Nernst plot" of the calculated coulometry of *S. acidocaldarius* Fd at pH 6.4, with the experimental values obtained represented by crosses.

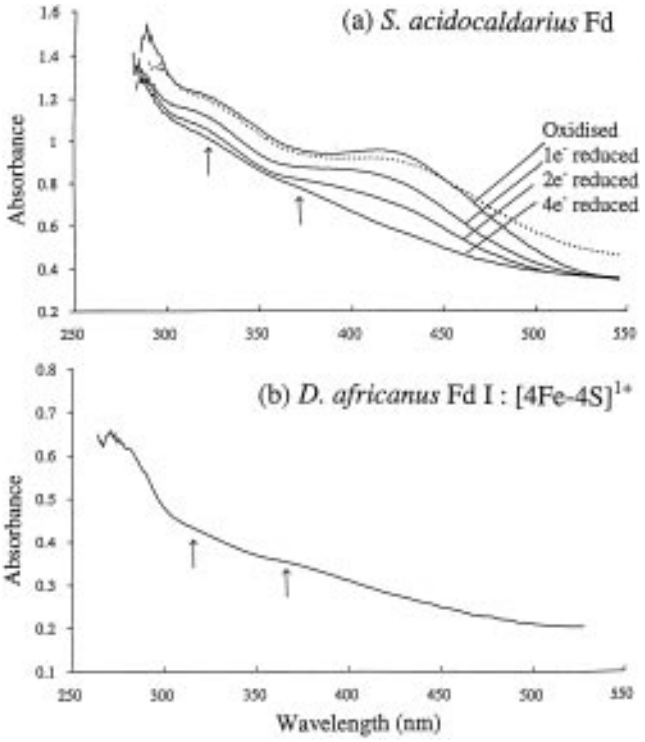

Figure 5. (a) UV/vis spectra of 80 μM *S. acidocaldarius* Fd in 20 mM Mes, 0.1 M NaCl, 0.1 mM EGTA, and 2 mM neomycin at pH 6.4. As-isolated, $1e^-$ reduced (−410 mV), $2e^-$ reduced (−633 mV), and $4e^-$ reduced (−882 mV). (- - -) Re-oxidized sample. (b) UV/vis spectra of 115 μM *D. africanus* Fd I in 0.1 M phosphate and 2 mM neomycin at pH 6.0. Reduced at −550 mV.

it was determined that the titrations were *reversible*; for example, following four-electron reduction at −857 mV, complete re-oxidation at −107 mV produced 3.8 electron equivalents. This reversibility was also observed spectroscopically, as described below.

Spectroscopy. 1. UV/Visible Absorbance. Figure 5a shows the UV/visible absorption spectrum of *Sa* Fd recorded after one, two, and four electron reductions of the same sample. There is a marked diminishing of the charge-transfer band at 408 nm after successive reductions, and the product has a pale straw color. The color changes provide a qualitative illustration of the changes in oxidation state of the ferredoxin from a system comprising formally five Fe(III) ($[3Fe-4S]^{1+}$ = 3Fe(III) and $[4Fe-4S]^{2+}$ = 2Fe(III)) through to just one Fe(III) ($[4Fe-4S]^{1+}$). The reversibility of the overall redox reaction was also

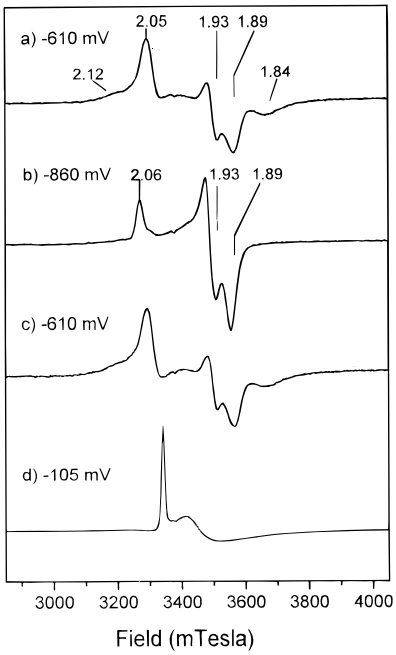

Figure 6. Perpendicular-mode EPR spectra of *S. acidocaldarius* ferredoxin samples prepared by direct electrochemistry on PGE electrodes: (a) 2-electron reduced at −610 mV; (b) 4-electron reduced at −850 mV; (c) solution in part b reoxidized by two electrons at −610 mV; (d) solution in part b reoxidized by four electrons at −105 mV. Conditions for all spectra were as follows: *Sa* Fd concentration = 80 μM in 20 mM Mes buffer, 0.1 M NaCl, 100 μM EGTA, 2 mM neomycin, at pH 6.4. Microwave frequency = 9.44 GHz. Microwave power = 2 mW. Temperature = 10.5 K for parts a, b, and c and 6.5 K for part d; gain = 2.0×10^5 (a and b), 2.5×10^5 (c), and 5.0×10^4 (d).

confirmed by electrochemical reoxidation; the dotted line represents the spectrum recorded after the sample was re-oxidized by four electrons. The increase in absorbance at higher wavelengths may reflect some sample deterioration after the redox cycle.

To compare with a protein for which the only visible chromophore is $[4Fe-4S]^{1+}$, a sample of a 4Fe Fd, in this case *Desulfovibrio africanus* Fd I,[60] was reduced by one electron to its $[4Fe-4S]^{1+}$ state. The spectrum is shown in Figure 5b and is similar in form to the 4-electron-reduced sample of *Sa* Fd in terms of the bleaching of the 400-nm region. Shoulders are observed at 375 and 325 nm for *Da* Fd I, compared to 370 and 320 nm for *Sa* Fd.

2. EPR. Perpendicular-mode X-band EPR spectra of electrochemically reduced samples of *Sa* Fd are shown in Figure 6. The upper trace (Figure 6a) corresponds to the 2-electron reduced form of the protein (potential for electrochemical reduction = −610 mV). The rhombic spectrum is attributable to the reduced $[4Fe-4S]^{1+}$ cluster with ground spin state $S = {}^1/_2$. In addition to the principal g-values ($g_1 = 2.05$, $g_2 = 1.93$, $g_3 = 1.89$), additional wings are observed on the high- and low-field sides of the main signal ($g = 2.12$ and 1.84) which are due to magnetic interactions with the reduced, paramagnetic ($S = 2$) $[3Fe-4S]^0$ cluster.[22] Thus, the $[4Fe-4S]^{1+}$ cluster acts as a probe of the electronic state of the [3Fe−4S] cluster. Double integration of this signal intensity at 18 K yields 1.0 ± 0.1 spin/mol and indicates that only the $[4Fe-4S]^{1+}$ cluster contributes to this region of the spectrum.

By contrast to this sharp signal, a very broad trough observed near zero field ("$g = 12$") indicates the presence of the reduced

(60) Hatchikian, E. C.; Cammack. R.; Patil, D. S.; Robinson, A. E.; Richards, A. J. M.; George, S. J.; Thomson, A. J. *Biochim. Biophys. Acta* **1984,** *784,* 40−47.

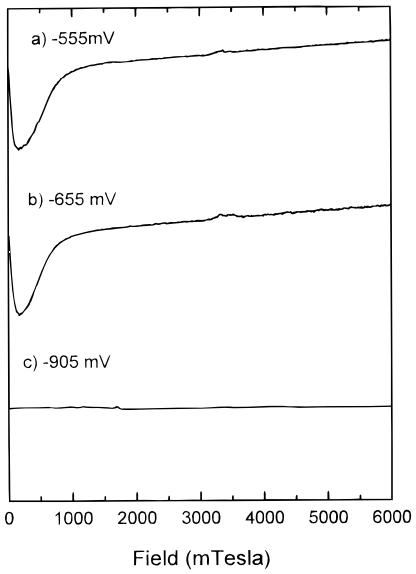

Figure 7. Parallel-mode EPR spectra of (a) 1-, (b) 2-, and (c) 4-electron reduced *S. acidocaldarius* ferredoxin samples prepared by direct electrochemistry on PGE electrodes. Conditions for all spectra were as follows: *Sa* Fd concentration = 80 μM in 20 mM Mes buffer, 0.1 M NaCl, 100 μM EGTA, 2 mM neomycin, at pH 6.4. Microwave frequency = 9.60 GHz; microwave power = 50 mW; temperature = 4.2 K; gain = 5.0×10^4.

$S = 2$ $[3Fe-4S]^0$ cluster. This signal has significant intensity in the parallel-mode EPR spectrum, whereas there is little or no intensity from the $S = {}^1/_2$ species in the $g \approx 2$ region. Figure 7 shows parallel-mode spectra for one- (7a) and two-electron (7b) reduced samples. Clearly, no change is observed in the $g = 12$ resonance when the [4Fe−4S] cluster is reduced to the paramagnetic 1+ state from the diamagnetic 2+ state.

Further reduction of the $[3Fe-4S]^0$ cluster at −860 mV leads to several changes in the EPR spectrum (Figure 6b). In the perpendicular mode spectrum of the reduced $[4Fe-4S]^{1+}$ cluster recorded at about 10 K, the "wings" at $g = 2.12$ and 1.84 have disappeared, although the remaining g-values of the rhombic spectrum are virtually unchanged ($g_{1'} = 2.06$, $g_{2'} = 1.93$, $g_{3'} = 1.90$). Double integration of this signal at 18 K also yields 0.9 ± 0.1 spin/mol, and thus no other species is contributing in this region at this temperature. Furthermore, in the parallel-mode spectrum of the 4-electron reduced ferredoxin, the broad trough at $g = 12$ has now disappeared (Figure 7c) after reduction at −905 mV, and no other signals are detected under the conditions used. The [3Fe−4S] cluster oxidation level and ground state spin have obviously changed. The relaxation properties of the $[4Fe-4S]^{1+}$ cluster are altered in the 4-electron reduced ferredoxin as compared to the 2-electron reduced sample, since the power for half-saturation at 15 K is decreased by approximately 50% ($P_{1/2}$ = 150 mW for 2e-, 80 mW for 4e-). The 4Fe cluster is thus now coupled to a more slowly relaxing form of the 3Fe cluster.

These effects are reversible: samples reduced by four electrons at −860 mV and subsequently reoxidized by two electrons to −610 mV showed recovery of the EPR spectrum of $[4Fe-4S]^{1+}$ identical to that of the form generated by initial reduction at −610 mV (Figure 6c). This shows that (as detected via its interaction with the $[4Fe-4S]^{1+}$ cluster) the 3Fe cluster reverts to the "0" oxidation state. Double integration of this signal yielded 0.8 spin/mol, thus confirming the integrity of the 4Fe cluster. Further reoxidation of the sample by two electrons, to −105 mV, led to the reappearance of the "$g = 2.01$" signal of $[3Fe-4S]^{1+}$ (Figure 6d). Again the recovery of spin concentration was almost quantitative (0.8 spin/mol as compared

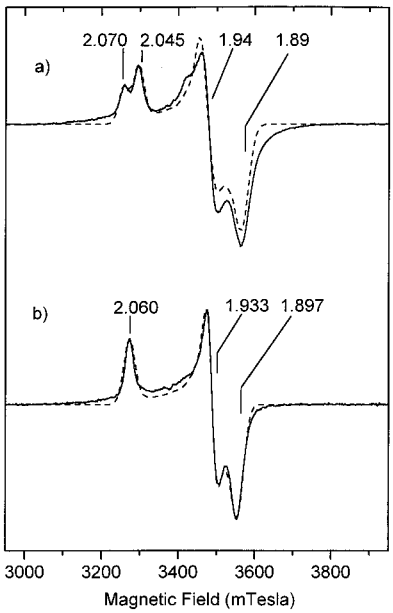

Figure 8. Perpendicular-mode EPR spectra (—) and computer simulations (- - -) of 4-electron reduced *S. acidocaldarius* ferredoxin samples prepared by direct electrochemistry on PGE electrodes: (a) temperature = 4.2 K, microwave power = 129 mW, gain = 2.0×10^4; (b) temperature = 20 K, microwave power = 2 mW, gain = 2.0×10^5. Conditions for both spectra were as follows: *Sa* Fd concentration = 255 μM in 20 mM Mes buffer, 0.1 M NaCl, 100 μM EGTA, 2 mM neomycin, at pH 6.4. Microwave frequency = 9.44 GHz. Modulation amplitude 10 G. The computer simulations were performed using the "EPR" program written by Frank Neese [Neese, F. *QCPE* **1995,** *15,* No. 136, 5]. The parameters were as follows: (a) species S1: $S = {}^1/_2$; g values, $g_1 = 2.0700$, $g_2 = 1.9327$, $g_3 = 1.8970$; Gaussian line widths, $w_1 = 15.5$ G, $w_2 = 15.0$ G; $w_3 = 19.0$G. Species S2: $S = {}^1/_2$; g values, $g_1 = 2.0450$, $g_2 = 1.9445$, $g_3 = 1.8880$; Gaussian linewidths, $w_1 = 15.5$ G, $w_2 = 15.0$ G; $w_3 = 20.0$G. (b) Species S3: $S = {}^1/_2$; g values, $g_1 = 2.0600$, $g_2 = 1.9327$, $g_3 = 1.8967$; Gaussian line widths, $w_1 = 17.5$ G, $w_2 = 15.0$ G, $w_3 = 19.0$G. Number of points = 1024; spectrometer frequency = 9.440 GHz.

to 1.0 spin/mol for the starting material). Thus, using the $[4Fe-4S]^{1+}$ cluster as a probe, the $[3Fe-4S]^0$ cluster is observed to undergo a reversible change of spin state upon "hyper-reduction" by two electrons.

The EPR spectrum of the $[4Fe-4S]^{1+}$ cluster in the 4-electron reduced ferredoxin showed an intriguing phenomenon under saturating conditions (Figure 8a). At very low temperature (4 K) and high microwave power, the signal in the $g \approx 2$ region is observed with g_1 apparently split into two peaks (2.04 and 2.07) and a shoulder at $g = 1.96$ which appears on the low-field side of g_2. It is obvious from variable-temperature and microwave studies that this represents a mixture of two species, with the $g_1 = 2.07$ species (S1) being more readily saturated than the $g_1 = 2.04$ species (S2). The spectrum of Figure 8a could be simulated approximately using a sum of two populations of $[4Fe-4S]^{1+}$ clusters, with S1 the slow-relaxing species ($g_1 = 2.070$, (Gaussian line width) $w_1 = 19.0$ G; $g_2 = 1.933$, $w_2 = 15.0$ G; $g_3 = 1.897$, $w_3 = 16.0$G) and S2, the rapidly relaxing species that is more readily observed under saturating conditions ($g_1 = 2.045$, $w_1 = 20.0$ G; $g_2 = 1.945$, $w_2 = 15.0$ G; $g_3 = 1.888$, $w_3 = 15.5$ G (for details of simulation see legend of Figure 8)). On the other hand, the $g = 1.94$ spectrum observed at 20 K could be adequately fitted using the parameters $g_1 = 1.897$, $w_1 = 19.0$ G; $g_2 = 1.933$, $w_2 = 15.0$ G; $g_3 = 2.060$, $w_3 = 17.5$ G (Figure 8b). It appears therefore that, allowing for small line shape changes at different temperatures, S1 is the species closest to the one observed at 20 K. The g values of S2 are also closer to those observed for the $[4Fe-4S]^{1+}$ cluster in the 2-electron reduced ferredoxin. Hence the "split" spectrum of Figure 8a could arise from a mixture of ferredoxins in different oxidation states, with the slow-relaxing $[4Fe-4S]^{1+}$ spectrum originating from the "hyper-reduced" ferredoxin containing $[3Fe-4S]^{2-}$ and $[4Fe-4S]^{1+}$ clusters, and the rapidly-relaxing $[4Fe-4S]^{1+}$ spectrum originating from the 2-electron reduced ferredoxin containing $[3Fe-4S]^0$ and $[4Fe-4S]^{1+}$ clusters. Note that the 4.2 K "split" spectrum under saturating conditions represents less than 10% of the intensity of the nonsaturating 4.2 K spectrum, and that it does not contribute to the unsplit spectrum observed at 20 K. This latter species yielded 0.9 spin/mol, representing at least 90% of the ferredoxin molecules. Therefore the fast relaxing species is a minor component of the sample, and it is consistent with partial re-oxidation of the ferredoxin to the stable 2-electron reduced state during transfer to the EPR tube. Another possibility is that a small proportion of the 3Fe cluster is present in the $[3Fe-4S]^{1-}$ state. However, this is very unlikely as the electrochemistry indicates that this species is unstable with respect to the 0 and 2− states. Furthermore, the ground spin state of the $[3Fe-4S]^{1-}$ cluster has been predicted to be $S = {}^5/_2$ with g values observed around 4.3.[20,38,41] We found no evidence for signals in this region. Finally, 4-electron reduced samples prepared for examination by MCD spectroscopy contained 50% (vol/vol) ethylene glycol to enable formation of optical quality glasses upon freezing. These samples showed the same EPR spectra as those prepared in aqueous buffer only.

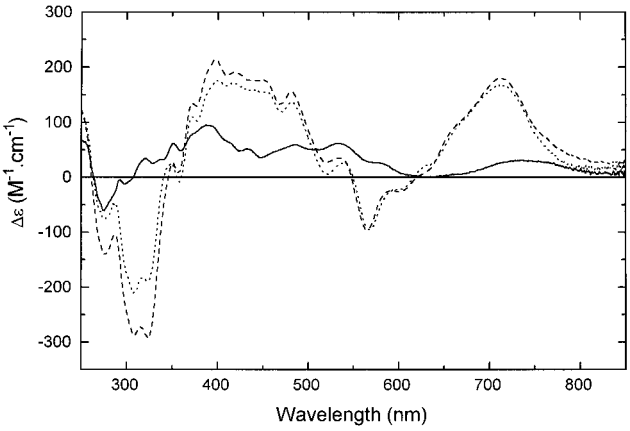

Figure 9. Low-temperature MCD spectra of *S. acidocaldarius* ferredoxin samples prepared by direct electrochemistry on PGE electrodes: (a) (···) 1-electron reduced at −510 mV, (b) (- - -) 2-electron reduced at −650 mV, (c) (—) 4-electron reduced at −850 mV. Conditions for all spectra were as follows: *Sa* Fd concentration = 80 μM in 50% (vol/vol) 20 mM Mes buffer, 0.1 M NaCl, 100 μM EGTA, 2mM neomycin, at pH 6.4/ethylene glycol. Path length = 1 mm; magnetic field = 5 T; temperature = 1.6 K.

3. MCD. The MCD spectra of the 1-electron, 2-electron, and 4-electron electrochemically reduced ferredoxin at pH 6.4 are shown in Figure 9. The intense spectrum of the one-electron reduced protein arises from the paramagnetic $[3Fe-4S]^0$ cluster with ground spin state $S = 2$ (Figure 9a). One of the most characteristic features is the broad, intense, MCD band centered at 710 nm ($\Delta\epsilon \approx 200$ M^{-1} cm^{-1} at 1.6 K and 5 T). The spectrum of the 2-electron reduced protein (Figure 9b) differs only slightly, due to additional contributions from the paramagnetic $S = {}^1/_2$ $[4Fe-4S]^{1+}$ cluster ($\Delta\epsilon \approx 40$ M^{-1} cm^{-1} at 1.6 K and 5 T in the 750 nm region).

It was possible to obtain further reduced samples by direct electrolysis at −860 mV, although we were unable to avoid some slight re-oxidation during transfer between the electrochemical cell and the MCD cell, as measured by some characteristic features of $[3Fe-4S]^0$ clusters observed in the

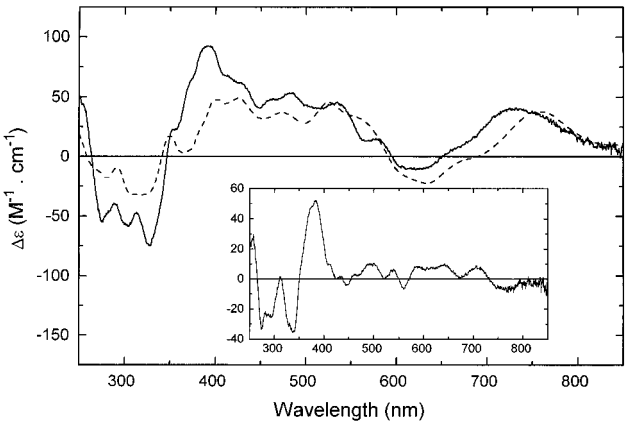

Figure 10. Low-temperature MCD spectra of *S. acidocaldarius* and *D. africanus* FdII ferredoxins: (a) (—) *Sa* Fd, 4-electron reduced at −850 mV, 1.6−45 K spectrum, conditions as in Figure 9; (b) (···) *Da* FdII, dithionite reduced $[4Fe-4S]^{1+}$ cluster. (Inset) Difference spectrum: [*Sa* Fd 4-electron reduced] − [*Da* FdII $[4Fe-4S]^{1+}$ 1-electron reduced] − [0.1 × *Sa* Fd $[3Fe-4S]^{0}$ 1-electron reduced], all spectra obtained at 1.6 K.

MCD spectrum (see below). At this potential we expect to observe the spectrum of the 4Fe cluster in the reduced (1+) state overlaid on the spectrum of the hyper-reduced $[3Fe-4S]^{2-}$ cluster. Several samples were produced and showed the same major features (Figure 9c). The most striking observation is the very low intensity of the spectrum as compared to that of the 2-electron reduced ferredoxin (Figure 9b). The maximum intensity in the 400−700-nm region has decreased from $\Delta\epsilon$ of $\approx$200 M^{-1} cm^{-1} to about 50 M^{-1} cm^{-1} for the temperature of 1.6 K and a magnetic field of 5 T. This spectrum is characteristic of $[4Fe-4S]^{1+}$ clusters with the $S = {}^1/_2$ ground spin state, as shown in Figure 10 where the 4-electron reduced *Sa* Fd MCD spectrum is compared with that of the $[4Fe-4S]^{1+}$ cluster of the 4Fe Fd II from *Desulfovibrio africanus*. However, some features are anomalous, such as the positive band at 390 nm (nearly twice as intense as the rest of the spectrum), the 550-nm dip that is typical of $[3Fe-4S]^{0}$ clusters, and the broad band maximum at 730 nm which is halfway between that of $[3Fe-4S]^{0}$ clusters (710 nm) and that of $[4Fe-4S]^{1+}$ clusters (750 nm).[49] To deconvolute the contributions, both the *Da* Fd II $[4Fe-4S]^{1+}$ spectrum and 10% of the 1-electron reduced *Sa* Fd $[3Fe-4S]^{0}$ spectrum (to account for some re-oxidation, as measured from the intensity of the 550-nm dip) were substracted from the 4-electron reduced spectrum.

The resulting MCD spectrum of the hyper-reduced $[3Fe-4S]^{2-}$ cluster is displayed in the inset of Figure 10 where it can be seen that there is little intensity at wavelengths longer than ca. 400 nm, and indeed no transitions have been detected with confidence in this region. This is consistent with the results from the absorption spectrum. Two MCD bands, one positive in sign at 370 nm and the other negative at 340 nm, with intensities of $\Delta\epsilon \approx 30-50$ M^{-1} cm^{-1} at 5 T and 1.6 K, appear to belong to the hyper-reduced cluster. The form of the spectrum bears a striking resemblance to that of the MCD spectrum of the Fe(II) state of the rubredoxin center, $[Fe^{II}(RS)_4]^{2-}$.[49] Oppositely signed bands are observed between 330 and 350 nm although the intensity is much higher, with $\Delta\epsilon \approx 1200$ M^{-1} cm^{-1} at 5 T and 1.6 K. Hence the MCD transition of the hyper-reduced $[3Fe-4S]^{2-}$ cluster lies in the region expected for Fe(II)−thiolate complexes. Charge-transfer transitions involving Fe(II) and S^{2-} are also expected to lie at similar energies. We therefore conclude that the MCD spectra are consistent with the assignment of the cluster to an all-Fe(II) form.

Discussion

Since our first report that the [3Fe−4S] cluster can undergo multiple electron transfers,[19] similar or related observations have been reported in the electrochemistry of an increasing number of [3Fe−4S]-containing ferredoxins.[21−28] The accumulating evidence points toward a generality of this formally all-Fe(II) state for the 3Fe cluster; however, to date, this observation has remained restricted to protein samples adsorbed on the electrode and therefore unsubstantiated by spectroscopic characterization of solution samples. Our finding that the $[3Fe-4S]^{0/2-}$ couple appears as an excellent diffusion-controlled process for solutions of *Sulfolobus acidocaldarius* ferredoxin has provided us with an opportunity to proceed further in the study of this highly reducing species. The similar behavior of couple C′ among all the ferredoxins in this study and the close correspondence between the results obtained for film and bulk solution studies of *Sa* Fd[22] lead us to conclude that the species formed in solution, by four-electron reduction of *S. acidocaldarius* ferredoxin, is very closely related, if not identical, to the products formed in the various protein films. As evidenced from its chemical reversibility at the electrode, and its longevity in solution, the species formulated as $[3Fe-4S]^{2-}$ is remarkably inert.

It was thus possible to characterize this species by various spectroscopic methods, as we were able to manipulate samples reduced by direct electrochemistry at very low potential in aqueous solutions. UV/visible and MCD spectroscopy showed that the 4-electron reduced *Sa* Fd has more Fe(II) character than the 2-electron reduced state, as evidenced from bleaching of the 400-nm absorbance and almost complete disappearance of the characteristic $[3Fe-4S]^{0}$ MCD spectrum. This is consistent with the disappearance of $RS^- \rightarrow$ core charge-transfer transitions normally found in the 350−550-nm region. The $S = 2$ ground spin state of the $[3Fe-4S]^{0}$ cluster has been described as resulting from antiferromagnetic coupling between a high-spin Fe(III) ion ($S = {}^5/_2$) and a valence delocalized Fe(II)−Fe(III) pair having a ground spin state $S = {}^9/_2$, the dimer spin resulting from double-exchange interaction.[41,61] This evidence, and the observation made for a serinate ligated form of *C. pasteurianum* $[2Fe-2S]^{1+}$ Fd having a $S = {}^9/_2$ ground spin state has led to the proposition that the 710-nm MCD band observed in the $[3Fe-4S]^{0}$ MCD spectrum originates from an intervalence charge-transfer transition associated with the valence-delocalized Fe(II)−Fe(III) fragment of the $[3Fe-4S]^{0}$ cluster having $S = {}^9/_2$.[62] The loss of this transition in the 4-electron reduced state of *Sa* Fd therefore correlates with the reduction of the $[3Fe-4S]^{0}$ cluster Fe(III) ions to the Fe(II) state. The change of oxidation state of the [3Fe−4S] cluster was also confirmed by EPR spectroscopy. Inter-cluster spin−spin coupling provides an indirect probe of the electronic state of the [3Fe−4S] cluster in *Sa* Fd because the distance between the two clusters must be relatively small (of the order of 10 Å) and therefore the paramagnetic $[4Fe-4S]^{1+}$ cluster ($S = {}^1/_2$, rhombic signal centered at $g = 1.94$) experiences the magnetic field of the [3Fe−4S] cluster. By monitoring the line shape of the signal at $g = 1.94$ it is possible to follow changes in the oxidation state of the [3Fe−4S] cluster. Indeed, the features observed at $g = 2.12$ and 1.83 in the 2-electron reduced ferredoxin disappear upon further reduction to the 4-electron reduced state. Further confirmation of a change in the cluster electronic state is the loss of the $g = 12$ signal for the 4-electron reduced sample as

(61) Papaefthymiou, V.; Girerd, J.-J.; Moura, I.; Moura, J. J. G.; Münck, E *J. Am. Chem. Soc.* **1987**, *109*, 4703−4710.
(62) Crouse, B. R.; Meyer, J.; Johnson, M. K. *J. Am. Chem. Soc.* **1995**, *117*, 9612−9613.

Table 3.

cluster oxidation state	$[3Fe-4S]^{1+}$	$[3Fe-4S]^{0}$	$[3Fe-4S]^{1-}$	$[3Fe-4S]^{2-}$
formal Fe oxidation state	3 Fe(III)	Fe(II) 2 Fe(III)	2 Fe(II) Fe(III)	3 Fe(II)
ground spin state	$S = {}^{1}/_{2}$[62]	$S = 2$[62,63]	$S = {}^{5}/_{2}$[38,20]	$S = 0, 1, 2, ...$

detected in the parallel-mode EPR spectrum. These techniques confirm independently that the $[3Fe-4S]^{2-}$ ground spin state is different from that of the $[3Fe-4S]^{0}$ cluster, itself an intrinsic and remarkably constant property of the cuboidal $[3Fe-4S]^{0}$ core, whether protein-bound or not (i.e. $S = 2$, with an axial zero-field splitting $D \approx -2.5$ cm^{-1} and rhombicity $E/D \approx 0.20-0.25$.[41,63,64]).

However we were not able to detect any new EPR signals, either in the perpendicular or parallel mode, that we could attribute unequivocally to the new $[3Fe-4S]^{2-}$ species (and thereby ascertain whether it is diamagnetic or paramagnetic). The only direct evidence for the all-Fe(II) cluster is the MCD peak around 370 nm, which could arise either from a thiolate or sulfide−Fe(II) ion charge-transfer transition. The magnetization characteristics (i.e. temperature and field dependence) of this band, containing information on the ground spin state, could not be measured because the MCD spectrum of $[4Fe-4S]^{1+}$ obscures this region.

Hence the identity of the ground spin state of the $[3Fe-4S]^{2-}$ species is still unclear. This should be an even spin system as all three iron atoms are high-spin Fe(II) ions ($S = 2$) (see Table 3) and should therefore lead to an integer ground spin state, irrespective of the coupling between isolated ions and/or a delocalized pair. Such a system would only be detectable in the parallel-mode EPR spectrometer if the zero-field splitting of levels were less than the microwave photon energy. We have been unable to detect any new signals so far, allowing for limitations in the sample concentration permitted by the electrochemical reduction method. Further parallel-mode EPR and Mössbauer experiments are required to establish the identity of the ground spin state of the $[3Fe-4S]^{2-}$ cluster.

A major observation made throughout these studies is the cooperative nature of the two-electron process, *i.e.* the $[3Fe-4S]^{1-}$ level appears to be by-passed during reduction and reoxidation. This cooperativity is unexpected and, to our knowledge, unprecedented for Fe−S clusters. In the absence of coulombic or structural compensation, successive electron-transfer reactions must always proceed anticooperatively due to the unfavorable accumulation of charge. Furthermore, we find strong evidence for the binding of a total of *three* protons at or close to the $[3Fe-4S]^{2-}$ cluster in each protein examined. This is in contrast with electrochemical studies of the small molecule analogue $[Fe_3S_4(LS_3)]^{3-}$, performed in the aprotic solvent acetonitrile, which show only the redox couples corresponding to 1+/0 and 0/1−, the latter appearing at extremely low potential, i.e. 0.93 V more negative than for the 1+/0 couple.[41] By rendering electron transfers electroneutral, accompanying proton-transfer steps alleviate the problem of charge accumulation,[35] but still do not provide a mechanism for *positive* cooperativity. One possible explanation is that the cluster undergoes a change in structure. However, of importance here are our observations that the reduction potentials of the $[3Fe-4S]^{0/2-}$ couple for all three ferredoxins and other examples at pH 7 are remarkably similar to each other (to within 20 mV). This argues against there being a major change in structure, since the various protein environments would be expected to offer different degrees of resistance to the redox reaction and this would be reflected in the free-energy change. We note the stark contrast with the ca. 0.5 V spread of potentials observed for the $[3Fe-4S]^{1+/0}$ couple (i.e. from −0.46 V for *Av* Fd I under alkaline conditions, to +0.06 V for beef heart mitochondrial succinate dehydrogenase[65]) in which just one electron is transferred without a proton. Consequently, in proposing that the insensitivity of the $[3Fe-4S]^{0/2-}$ reduction potential to the surrounding protein environment is explained by the reduction process being electroneutral, we must also postulate that the cooperativity originates in more subtle electronic/protonic characteristics of the different oxidation levels. Considering the overall H^+/e^- stoichiometries and the marked attenuation of couple C′ above neutral pH, we thus suggest that some special stability is associated with the overall uptake of *three* protons at this cluster.

The question of where the protons bind is difficult to answer. There are three documented examples[21,22,30] where it has been shown that the [3Fe−4S] cluster can take up *one* proton when reduced to the $n = 0$ state. The changes observed in the MCD spectrum are similar in each case and provide compelling evidence that protonation directly perturbs the cluster itself.[21,29,66] Furthermore, studies on the D15N mutant of *A. vinelandii* Fd I show marked retardation of redox interconversion of the $[3Fe-4S]^{0/2-}$ couple[21] attributable to the much slower proton transfer between cluster and bulk solvent when an aspartate (D15) that is believed to mediate this proton transfer[33] is changed to asparagine. One hypothesis for the proton binding site, supported by studies on non-protein Fe−S models[16] is that one of the inorganic μ_2 sulfides becomes protonated; however, neither crystallographic nor Mössbauer studies could detect structural changes or unambiguously locate the protonation site.[34] Hydrogen bonding between protein amide residues and inorganic sulfides is a common feature of cluster binding domains and may be important in influencing reduction potentials.[67]

For the hyper-reduced cluster, an interesting, although speculative possibility is that the three inorganic μ_2 -sulfur atoms at the "vacant corner" of the 3Fe cluster present a trigonal planar set of electron-rich donor orbitals and thus provide a host capable of stabilizing triangular "guest" species. Two interesting possibilities are H_3O^+ and H_3^{n+}. For example, single protonation of the $[3Fe-4S]^{0}$ cluster could involve addition of the pyramidal hydroxonium ion, H_3O^+, to cap the corner of the cluster, each hydrogen atom forming a bond to one μ_2-sulfur atom. Simple model studies show that reasonable S···H−O distances are produced if the hydroxonium ion caps the corner. However, the presence of a capping O-atom is not revealed by crystallography of the [3Fe−4S] form *Av* Fd I at pH 6;[34b] furthermore, there is no obvious means of adding two additional H^+ in a cooperative manner to stabilize $[3Fe-4S]^{2-}$. The

(63) Emptage, M. H.; Kent, T. A.; Huynh, B. H.; Rawlings, J.; Orme-Johnson, W. H.; Münck, E. *J. Biol. Chem.* **1980,** *255,* 1793−1796. Huynh, B. H.; Moura, J. J. G.; Moura, I.; Kent, T. A.; LeGall, J.; Xavier, A. V.; Münck, E. *J. Biol. Chem.* **1980,** *255,* 3242−3244.

(64) Thomson, A. J.; Robinson, A. E.; Johnson, M. K.; Moura, J. J. G.; Moura, I.; Xavier, A. V.; Le Gall, J. *Biochim. Biophys. Acta* **1981**, *670,* 93−100.

(65) Ackrell, B. A. C.; Johnson, M. K.; Gunsalus, R. P.; Cecchini, G. In *Chemistry & Biochemistry of Flavoenzymes;* Müller, F., Ed.; CRC Press: Boca Raton, FL, 1992. Hederstedt, L.; Ohnishi, T. In *Molecular Mechanisms in Bioenergetics*; Ernster, L., Ed.; Elsevier: New York, 1992; pp 163−198.

(66) Stephens, P. J.; Jensen, G. M.; Devlin, F. J.; Morgan, T. V.; Stout, C. D.; Martin, A. E.; Burgess B. K. *Biochemistry* **1991,** *30,* 3200−3209.

(67) Backes, G.; Mino, Y.; Loehr, T. M.; Meyer, T. E.; Cusanovich, M. A.; Sweeney, W.V.; Adman, E. T.; Sanders-Loehr, J. *J. Am. Chem. Soc.* **1991,** *113,* 2055−2064.

suggestion that three protons might bind cooperatively as a coordinatively-stabilized H_3^{n+} entity is prompted by the intrinsic stability of the triangular H_3^+ ion in the gas phase (H_2/H^+ dissociation energy 420 kJ mol^{-1}).[68] In the condensed phase, this might be stabilized by a ligand having the appropriate geometry and an environment lacking competing bases. Electron withdrawal should create an entity with retention of the required trigonal structure, and electron delocalization across the cluster could stabilize the $[3Fe-4S]^{2-}-3H^+$ species. Indeed, in terms of charge alone, the limiting hypothetical "H_3^{3+} species" is formally equivalent to Fe^{3+} which of course is known to form a stable cluster with three Fe(II) and four sulfides in the commonly-occurring $[4Fe-4S]^{1+}$ species. Special stability associated with *coordinated* H_3^{n+} could explain why formation of the all-Fe(II) state is a cooperative two-electron reaction, bypassing the "super-reduced" state $[3Fe-4S]^{1-}$, and not necessitating protein-sensitive structural changes. The "1−" species, with presumably just *two* protons, might lack the orbital overlap stability achieved by the presence of a third proton. Hence we suggest two special (and not implausible) processes for protonation of the $[3Fe-4S]^0$ and $[3Fe-4S]^{2-}$ clusters which, respectively, maintain electroneutrality with the oxidized state, $[3Fe-4S]^{1+}$. Neither of these mechanisms confer electroneutrality on $[3Fe-4S]^{1-}$ and this state is not observed.

The formation of an all-Fe(II) [3Fe−4S] cluster, stabilized by protonation, has a wider relevance for the function of Fe−S clusters in biology. First, it illustrates that the [3Fe−4S] cluster has the capability to act as a multiple electron−proton transfer agent, which, if this is not simply a phenomenom of the proteins in this study, has wider ramifications for the role of Fe−S clusters in biology. For example, this has implications for enzymes such as nitrogenase,[6] and the Fe-only hydrogenases[69] whose reaction mechanisms also involve the coupling of protons and electrons, and where Fe−S clusters are the only prosthetic groups available. Second, it calls into question the relevance of highly reducing species in biology. The physiological function, if any, for the $[3Fe-4S]^{0/2-}$ couple is unknown; direct electrochemistry, however, enables the detection and study of systems that are reactive and far from equilibrium. Strong reductants could well be important in some transient way in biological systems: for example, chlorophyll P_{700} in Photosystem I generates a highly reducing species having a potential lower than −1 V;[70] in addition, "Fe−S cluster X" occurring in the same photosystem has an exceptionally negative reduction potential, −705 mV,[71] as does a center (Center B) in the W−FeS enzyme, aldehyde oxidoreductase from *P. furiosus*.[72] We should consider also that under more acidic conditions (pH ≤4) the reduction potential for the $[3Fe-4S]^{0/2-}$ couple becomes comparable with that of many $[4Fe-4S]^{2+/1+}$ clusters. Third, the existence of a relatively stable asssembly of Fe(II) and (hydro)sulfide may be relevant in mechanisms for formation of Fe−S clusters *in vivo* where the kinetically available form of iron is Fe(II), not Fe(III), and available inorganic sulfide is not S^{2-}, but HS^-. Assembly of Fe−S clusters might in some cases involve a species composed entirely of Fe(II) ions in conjunction with (predominantly) HS^-. By formulating the hyper-reduced cluster as $[3Fe^{II}-3(SH^-) + S^{2-}]$, it is apparent that such a species could provide a relatively stable intermediate in the course of assembly of cubane-type clusters.

Acknowledgment. This research was supported by the US National Science Foundation (MCB-9118772 to F.A.A.), by the UK Engineering and Physical Sciences (EPSRC) and Biological and Biochemical Research Councils (BBSRC) (Grants GR/J84809 to F.A.A. and GR/H50753 to A.J.T.), and by a NATO collaborative research grant, CRG9003 (F.A.A., A.J.T.). We are grateful to the European Union for support via a MASIMO grant (ERBCHRXCT920072 to A.J.T.) and the generic project "Biotechnology of Extremophiles" (B102-CT93-0274 to A.J.T.). We thank Professor Barbara Burgess for providing a sample of *Azotobacter vinelandii* ferredoxin.

JA961465L

(68) See, for example; Carrington, A., McNab, I. R. *Acc. Chem. Res.* **1989,** *22,* 218−222 and refences therein.

(69) Adams, M. W. W. *Biochim. Biophys. Acta* **1990,** *1020,* 115−145.

(70) Golbeck, J. H.; Bryant, D. A. *Curr. Top. Bioenerg.* **1989,** *16,* 83−177.

(71) Charmorovsky, S. K.; Cammack R. *Photobiochem. Photobiophys.* **1982,** *4,* 195−200.

(72) Mukund, S., Adams. M. W. W. *J. Biol. Chem.* **1991,** *266,* 14208−14216.